Int. J. Electrochem. Sci., 16 **(2021)** Article Number: 211212, doi: 10.20964/2021.12.08

International Journal of
ELECTROCHEMICAL
SCIENCE
www.electrochemsci.org

Effects of counter-ions on the electropolymerization behaviors and properties of polyaniline

Han Xu[*], *Xiaonan Wu*

Department of Chemical Engineering, Chengde Petroleum College
Chengde 067000, Hebei, P. R. China
[*]E-mail: cdpc_xuh@163.com

Received: 16 August 2021 / *Accepted:* 25 September 2021 / *Published:* 10 November 2021

Conductive polymer of polyaniline (PANI) was prepared by potentiostatic electropolymerization technique onto Au at 25℃ in a series of solutions containing NO_3^-, SO_4^{2-}, Cl^-, ClO_4^- and PO_4^{3-}, respectively. The effects of different counter-ions on the electropolymerization behaviors and capacitive behaviors of PANI films were investigated by cyclic voltammetry (CV) and electrochemical impedance spectroscopy (EIS) electrochemical measurements. As a result, the difficulty of electropolymerization of aniline in electrolytes containing different kinds of counter-ions from high to low is in the order: $NO_3^- > SO_4^{2-} > ClO_4^- > Cl^- > PO_4^{3-}$, while the rate of electropolymerization of aniline in electrolytes containing different kinds of counter-ions from high to low is in the order: $SO_4^{2-} > NO_3^- > Cl^- > ClO_4^- > PO_4^{3-}$. The order of the conductivity of pAn films obtained in solutions containing different counter-ions from high to low is: PANI/HNO_3 > PANI/H_2SO_4 > PANI/HCl > PANI/$HClO_4$> PANI/H_3PO_4. The order of the charge storage ability of PANI obtained in different solutions from high to low is: PANI/H_2SO_4> PANI/HNO_3 > PANI/HCl > PANI/$HClO_4$> PANI/H_3PO_4.

Keywords: polyaniline; electropolymerization; counter-ions; EIS; capacitive behaviors.

1. INTRODUCTION

With the discovery in 1960 of intrinsically conducting polymers, polyaniline has received a great deal of interest as its ease of synthesis, low cost monomer, tunable properties, and high stability in water and air. Results of a great deal of investigations have shown that PANI has potential applications in multidisciplinary fields, such as ion-exchange material[1], electrode for rechargeable batteries[2,3], anode for microbial fuel cells[4], capacitor or energy storage devices[5-8], membranes of gas separations[9,10], conductive adhesive[11], and so on.

Different ways to produce pAn have been demonstrated, including chemical[12,13],

electrochemical[14-16], template[17-19], enzymatic [20,21], plasma[22,23], photo[24,25], and a number of other special methods. While electrochemical polymerization which is again subdivided into potentiostatic, galvanostatic and potential cycling methods has obtained much more attentions due to the convenience of controlling the thickness, morphology and electrooptical properties of pAn film by adjusting the applied mode of electropolymerzing potential[26-28].

Except for the electropolymerization parameters, kinds of counter-ions used in the electrolyte also show significant impact on the morphology[29] and properties[30] of PANI. Hao et al. [31] found that the properties and electrochemical behavior of electropolymerized PANI could furtherly be changed by exchanging the counter-ions in the film using a CV method. The authors concluded that both the original and the redoping counter ions played an important role in the electrical and electrochemical properties of PANI. However, the morphology did not change after exchanging the counter ions. And the electro-optical property of PANI is also determined by the original dopant ions using in the electropolymerization. This maybe explained by a 'size memory effect' proposed by Lapkowski and Vieil [32], which means that once doped, the PANI film kept the memory of the size of the doping anion and can be only re-doped by comparable or smaller anions. Based on the fact above, effects of the original counter ions on the electropolymerization process of PANI are necessary to be discussed. So we investigated the effect systematically by means of electrochemical measurements as CV and EIS. The effect on electrical properties of the electropolymerized PANI films were also discussed. All the results were presented in this paper.

2. EXPERIMENTAL

2.1. Solutions

Aniline, nitric acid (HNO_3), sulfuric acid (H_2SO_4), hydrochloric acid (HCl), perchloric acid ($HClO_4$), phosphoric acid (H_3PO_4), potassium nitrate (KNO_3), potassium sulphate (K_2SO_4), potassium chloride (KCl), potassium perchlorate($HClO_4$) and potassium phosphate(K_3PO_4) were analytical grade and obtained commercially. All electrolytes were prepared with redistilled water. Five kinds of solutions named solution (i) ~ solution (v) were used. The compositions of each solution are shown in Tab.1.

Table 1. Composition of electrolytes for electrochemical measurements and electropolymerization

Solution	aniline	HNO_3	KNO_3	H_2SO_4	K_2SO_4	HCl	KCl	$HClO_4$	H_3PO_4	K_3PO_4
i	0.1 M	1 M	1 M	——	——	——	——	——	——	——
ii	0.1 M	——	——	0.5 M	0.25 M	——	——	——	——	——
iii	0.1 M	——	——	——	——	1 M	1 M	——	——	——
iv	0.1 M	——	——	——	——	——	——	1 M	——	——
v	0.1 M	——	——	——	——	——	——	——	1 M	0.25 M

2.2. Electrochemical measurements

The electrochemical measurements were carried out with a PAR Model 2273 electrochemical working station at 25℃. A standard three-electrode system was employed as the electrochemical cell, which was consisted of a working electrode, a Pt plate as the counter electrode, and a saturated calomel electrode (SCE) as the reference electrode. A bare Au plate or a PANI film covered Au plate (named as PANI film) were used as the working electrode, separately. The working area of both working electrodes is 1 × 1 cm^2. The Au plate was mechanically polished to ensure constant electrode area, and then degreased with acetone, electrochemically degreased and rinsed with redistilled water in order to ensure a clean surface. PANI film covered Au plate was prepared by electropolymerization of anilines on the treated Au plate at 0.9 V for 5 min in solution (i) ~ solution (iv) or at 0.7 V in solution (v), respectively. The obtained film was named as PANI/HNO_3, PANI/H_2SO_4, PANI/HCl, PANI/$HClO_4$ and PANI/H_3PO_4, respectively. All the potentials were measured and indicated against SCE. Solutions were not stirred during all the electrochemical measurements.

The cyclic voltammograms were recorded with sweep rate 20 mV/s. The scanning ranges depended on the solution. The electrochemical impedance spectroscopy (EIS) measurements were carried out in a frequency range of 10^{-2} Hz ~ 10^5 Hz at different polarizing potentials and the applied potentials amplitude was 5 mV. The EIS data were further analyzed by ZSimpWin software.

3. RESULTS AND DISCUSSION

3.1. Cyclic voltammetry analyses

The electropolymerizaition behaviors of polyaniline in solutions containing different counter-ions were investigated by means of cyclic voltammetry.

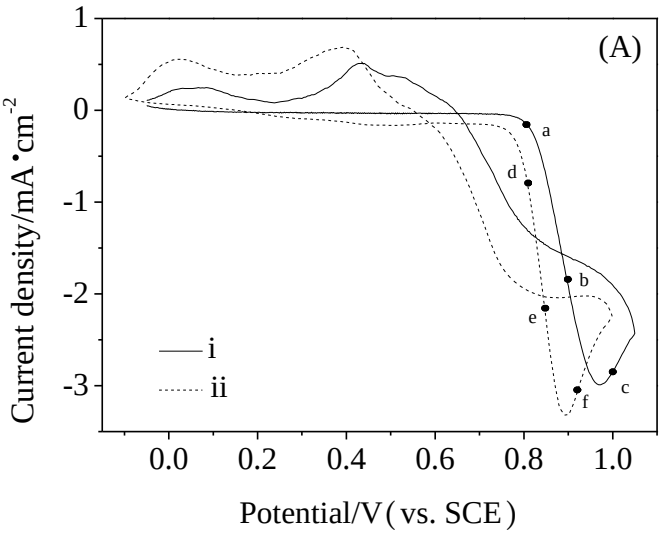

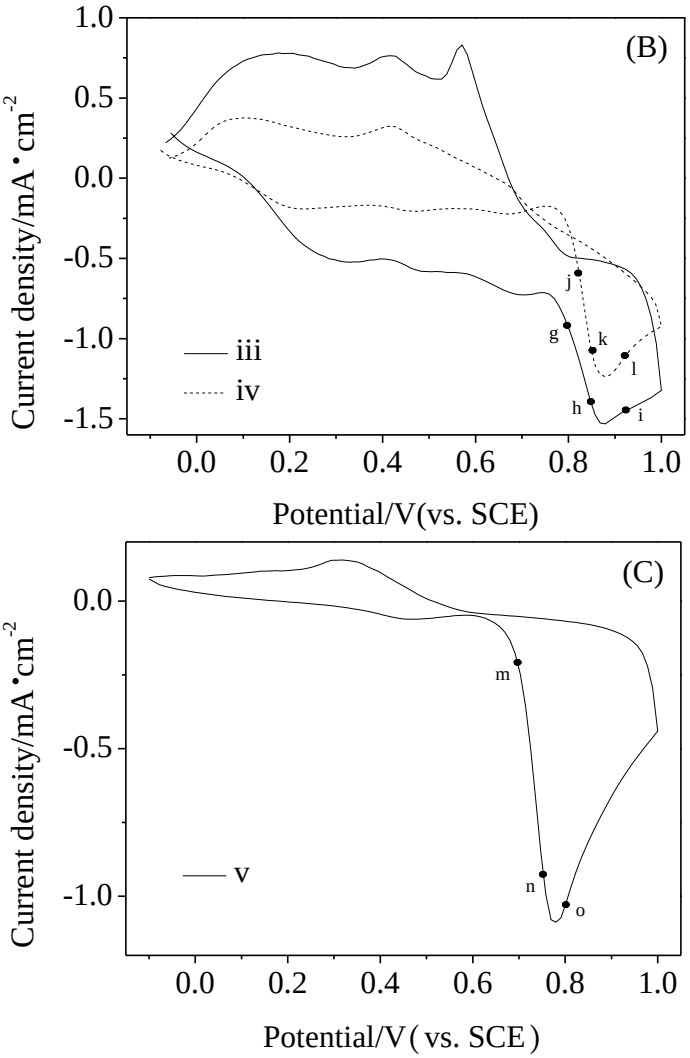

Figure 1. Cyclic voltammograms of aniline on Au plate in different solutions. (A): solution (i) and solution(ii), (B): solution (iii) and solution (iv), (C): solution (v) ,scanning rate = 20 mV/s.

The cyclic voltammograms of Au plate in each solution were measured and showed in Fig. 1. All the cyclic voltammograms are the first recorded cycle. Curve (i) in Fig. 1A show the cyclic voltammograms on Au electrode in solution (i). It can be seen that there are four peaks on curve (i), including only one oxidation peak locates at 970 mV and three reduction peaks locate at 530 mV, 430 mV and 60 mV, respectively. The formation of PANI film with green color on the Au electrode can be observed when the potential scans positively to 800 mV, which indicates that the monomer aniline are electrochemically oxidized at 800 mV or even positive potential. Therefore, the only oxidation peak on this curve is corresponding to the oxidation of aniline to radical and then grow into PANI film [33]. The formed PANI film will be further oxidized as the electrode potential scanning to a higher potential [34]. And the peaks on the cathodic branch are considered to be ascribed to the reduction of the oxidized PANI, like from polaron states to PANI, pernigraniline (P) to emeraldine (E) or from emeraldine (E) to leucoemeraldine (L), respectively[31, 33].

Curve (ii) of the CV curve recorded in solution (ii) shows similar peak shape with that in curve (i). The most significant difference between the two curves is that there are two oxidation peaks on curve (ii). As the formation of PANI film on the electrode was observed when the potential is higher than 800 mV, the oxidation peak locates at 895 mV is identified as the oxidation of aniline to radical. While the other oxidation peak locate at 450 mV is assumed to be the oxidation of the dimers formed in the electrolyte chemically [33]. And the peaks on the cathodic branch are also considered to be ascribed to the reduction of different states of PANI.

Curve (iii) and Curve (iv) in Fig.1B show the cyclic voltammograms on Au electrode recorded in solution (iii) and solution (iv), respectively. Both the peak potential and peak shape of these two curves are similar in some degree. And it seems that more complicated reactions occured in the two solutions involved due to more peaks appear on the two curves than that on curve (i) and (ii). It can be seen in this figure that there are seven peaks on curve (iii), including four oxidation peaks locate at 320 mV, 500 mV, 700 mV, 875 mV, and three reduction peaks locate at 570 mV, 420 mV and 175 mV, respectively. While there are six peaks on curve (iv), including four oxidation peaks locate at 220 mV, 470 mV, 670 mV, 880 mV, and two reduction peaks locate at 420 mV and 100 mV, respectively. The formation of green film on Au electrode which can only be observed when the electrode potential scans positively to the last oxidation peak leads to the conclusion that the oxidation peaks locate at 875 mV and 880 mV respectively on both curves are corresponding to the oxidation of aniline. Other oxidation peaks on both curves are assumed to be ascribed to the oxidation of different dimers or oligomers generated in the electrolyte chemically [33], and will not be the focus of this paper due to our current interest is the growth of PANI film from aniline. We proposed that the formation of dimers or oligomers may be associated with the chlorine element in the electrolytes based on existing experimental phenomenon, and will do further investigate in future work. The cathodic peaks on the two curves are similar to that on curve (i) and (ii) relatively. Then the peaks appear at 420 mV and 175 mV on curve (iii) and the peaks appear at 420 mV and 100 mV on curve (iv) are all considered to be the reduction of oxidized PANI film. While the extra cathodic peak at 570 mV on curve (iii) perhaps related to the reaction of solution species like chlorine [31].

Curve (v) in Fig.1C shows the cyclic voltammogram on Au electrode recorded in solution (v). It can be seen that there are three peaks on this curve, including two oxidation peaks locate at 460 mV, 780 mV, and one reduction peak locates at 320 mV, respectively. The formation of green film on the Au electrode can only be observed when the electrode potential scans positively to the last oxidation peak. Therefore, it can be concluded that the oxidation peak locates at 780 mV is corresponding to the oxidation of aniline. And the other oxidation peak on this curve may be corresponding to the oxidation of the dimers. While the peak presents on cathodic branch of the cyclic voltammogram is also considered to be ascribed to the reduction of PANI.

Because of our interest is the formation of PANI film from monomer aniline, the anodic peaks corresponding to the oxidation of aniline on the five CVs are investigated in detail. The peak potentials and peak currents of each oxidation peak are shown in Tab. 2. It can be obtained from Tab. 2 that the difficulty of the oxidation of aniline in electrolytes containing different kinds of counter-ions from high to low is in the order: NO_3^-> SO_4^{2-}> ClO_4^-> Cl^-> PO_4^{3-}, while the rate of the corresponding oxidation reaction in different electrolytes from high to low is in the order: SO_4^{2-}> NO_3^-> Cl^-> ClO_4^-> PO_4^{3-}.

Table 2. Peak potentials and peak currents of electropolymerization peaks on the first recorded cycle of cyclic voltammograms in electrolytes containing different kinds of counter-ions.

	NO_3^-	SO_4^{2-}	Cl^-	ClO_4^-	PO_4^{3-}
Peak potential(mV)	970	895	875	880	780
Peak current($mA \cdot cm^{-2}$)	-2.99	-3.35	-1.53	-1.24	-1.10

3.2 Electrochemical impedance spectroscopy analyses

Electrochemical impedance spectroscopy (EIS) has been regarded as a very practical tool for getting more information about the kinetics of redox process. In order to investigate the resistances of the electropolymerization reactions on Au in electrolytes containing different kinds of counter-ions, the EIS were obtained at different potentials in solution (i) ~ solution (v) corresponding to points a ~ o in Fig. 1 and the Nyquist and Bode plots are shown in Fig. 2.

The EIS plots measured on Au in solution (i) are shown in Fig.2A and Fig. 2A'. It can be found that the Nyquist plot measured at 0.8 V in solution (i) shows one big semicircle in high frequency range which can be attributed to the oxidation of aniline to radical cation on Au substrate. Both of the Nyquist plots measured at 0.9 V and 1.0 V in solution (i) are consisted of a semicircle in high frequency region and a straight line in low frequency region, and the semidiameters of the semicircles becomes smaller while the potential moves positively. It indicates that the rate controlling step varies from electropolymerization reaction to monomer diffusion when the electrode potential is positive enough.

As described by Mandic et al., the formed PANI films was compact initially, but grew into different shapes depending on the counter ions [35]. Change of the film morphology and thickness is also reflected in the impedance response of PANI films. Huyen et al. proposed that the main reason for this phenomenon is the variety of film porosity [36]. In our study, the PANI film obtained at high potentials became porous under diffusion control. We consider this is the origin of the appearance of an inductive valley in high frequency reigon on Bode plot measured at 1.0 V based on the analysis of Huyen. Bode plot measured at 0.8 V in solution (i) (Fig.2A', 0.8 V) shows one time constant which may be corresponding to the oxidation of aniline to radical cation. While Bode plots measured at 0.9 V and 1.0 V in solution (i) （Fig.2A', 0.9 V, 1.0 V）show two time constants. According to our existing analysis [37], the first one is corresponding to the oxidation of aniline to radical cation, while the second one is corresponding to the oxidation of formed PANI film. As the oxidation of monomer aniline is more difficulty than that of the PANI film, it can be predicted that the arc in the Nyquist plot is related to the electrochemical oxidation of aniline rather than the oxidation of PANI film. And the radius of the arc corresponding to the oxidation of PANI is too small to be identified in the plot.

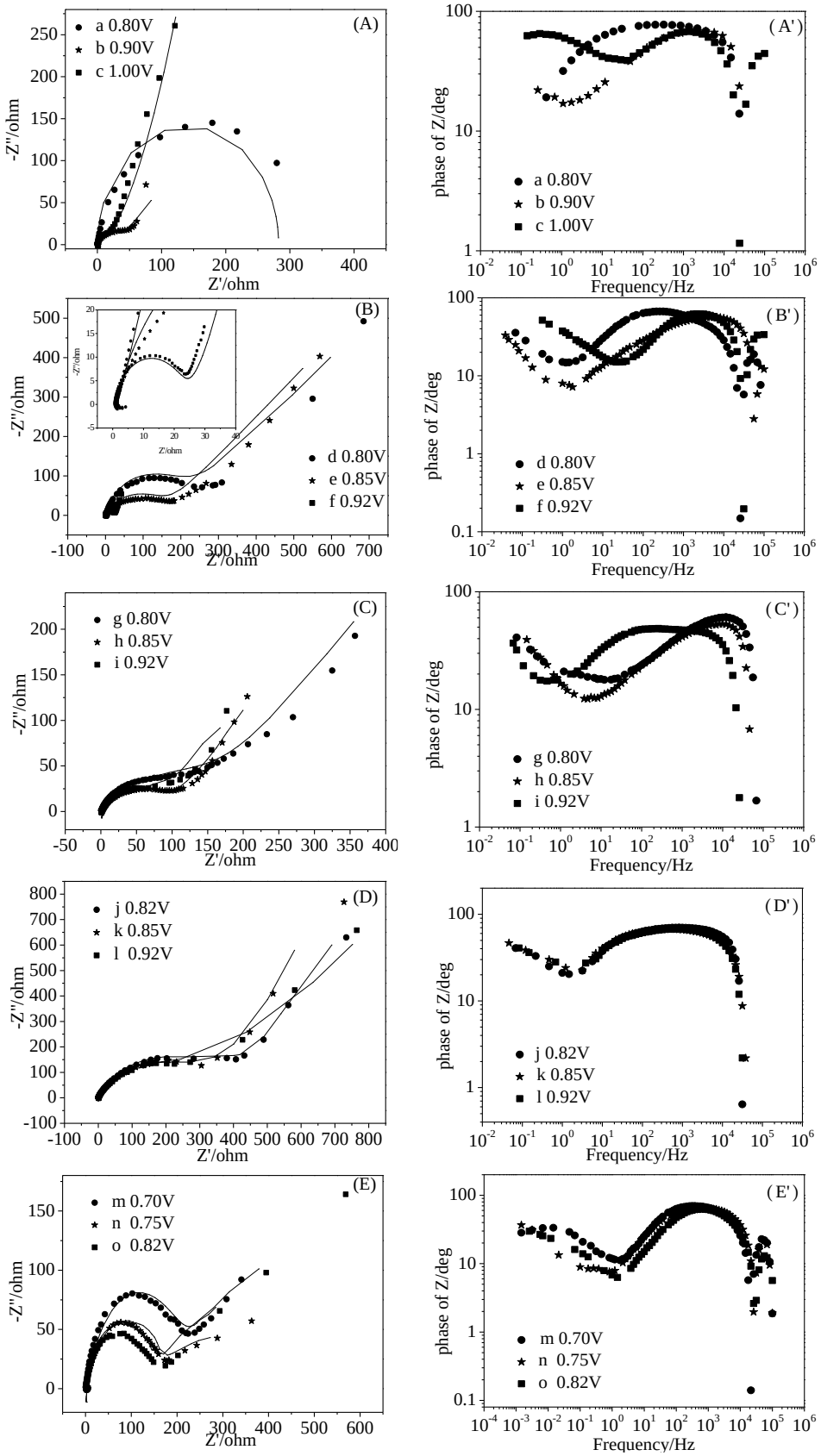

Figure 2. EIS plots measured on Au plate at different potentials in different electrolytes corresponding to point a ~ o in Fig.1. (A) ~ (E) are Nyquist plots, (A') ~ (E') are Bode plots. A, A': solution (i), B, B': solution (ii), C, C': solution (iii), D, D': solution (iv), E, E': solution (v). Points: tested data, line: simulated results.

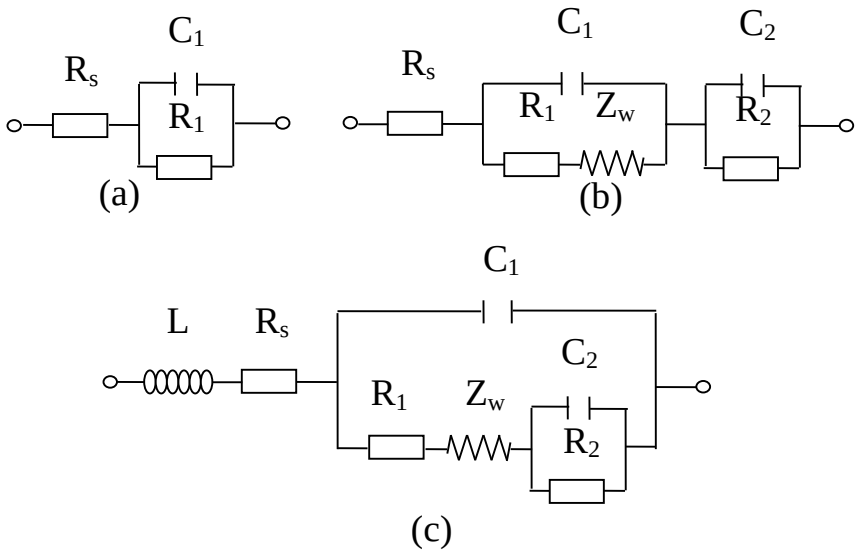

Figure 3. Equivalent circuits used to simulate the EIS plots in Figure 2A. (a) 0.8 V.(b) 0.9 V.(c) 1.0 V.

Based on the analysis above, The Nyquist plot was simulated by corresponding equivalent circuits shown in Fig. 3. Where, L represents the formation of porous structure, R_s accounts for the uncompensated solution resistance between the reference electrode to the working electrode, C_1 and R_1 are the double layer capacitance and charge transfer resistance of the oxidation of aniline to radical cation on the Au electrode surface, respectively. C_2 and R_2 are the double layer capacitance and charge transfer resistance which can be ascribed to the oxidization of PANI film, respectively. Z_w is the Warburg impedance due to the monomer diffusion in the solution. The appearance of the circuit element of L in the equivalent circuit is coincide with the valley shown in Bode plot.

Be distinguished with the Nyquist plots of solution (i), all the Nyquist plots of solution (ii) show an extra inductive arc in extremely high frequency region as shown in Fig. 2B. Correspondingly, an inductive valley appears on all the Bode plots shown in Fig. 2B'. Both the phenomena could be attributed to the porous structure of the formed PANI as confirmed by our earlier work [29]. Meanwhile, all Bode plots show two time constants, and may be caused by the electrochemical oxidation of monomer aniline and PANI film, respectively. And the capacity arc on Nyquist plot is ascribed to the oxidation of aniline for the same reason analyzed above.

Nyquist plots in Fig.2B are also simulated using corresponding equivalent circuits shown in Fig.4. Where, L and R_L are related to the formation of porous structure, R_s accounts for the uncompensated solution resistance between the reference electrode to the working electrode [39, 40], R_1 and R_2 are the charge transfer resistance of the electrochemical oxidation of monomer aniline and PANI film, respectively. Q_1 reflects the charging of Au/solution double layer at the base of the pores of the initial formed PANI film [36]. Q_2 arises from the PANI pseudocapacitive redox reaction [31, 36]. Z_{w1} and Z_{w2} are the Warburg impedance due to the monomer diffusion in the solution. We use a constant phase element (Q) instead of a capacitor (C) to obtain the best-fit. A Q is related to a capacitor through the relationship $C=Q^n$, where n can have a value between 0 and 1 [36]. n values less than 1 are seen for the charging of a rough and/or porous electrode surface [38]. From the variety of equivalent circuits, it can

be concluded that the oxidation of aniline may be a fast reaction as be controlled by the diffusion of monomer at a lower potential, while the growth and oxidation of PANI may be a slower reaction as be controlled by the diffusion at a much higher potential.

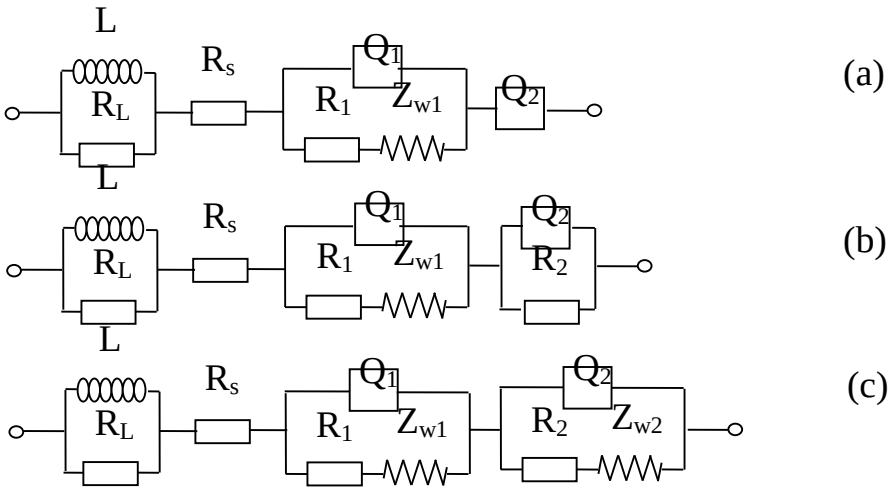

Figure 4. Equivalent circuits used to simulate the EIS plots in Figure 2B. (a) 0.8 V.(b) 0.85 V.(c) 0.92 V.

Similar Nyquist plots were obtained in solution (iii) ~ (v) as shown in Fig. 2C ~ 2E. All Nyquist plots are consisted of one big capacitive are in high frequency range and a straight line in low frequency region, and the radius of the arcs become smaller while the potential moves positively. It indicates that the rate controlling step varies from electrochemical oxidation to monomer diffusion when the electrode potential is positive enough. The capacity arc on Nyquist plot is considered to be the oxidation of aniline for the same reason analyzed above.

All Bode plots of solution (iii) show two time constants as seen in Fig. 2C'. Similar as analyzed above, the first one is corresponding to the capacitance and resistance of the oxidation of monomer aniline, while the second one is corresponding to the double layer capacitance and charge transfer resistance which arise from the oxidation of PANI film.

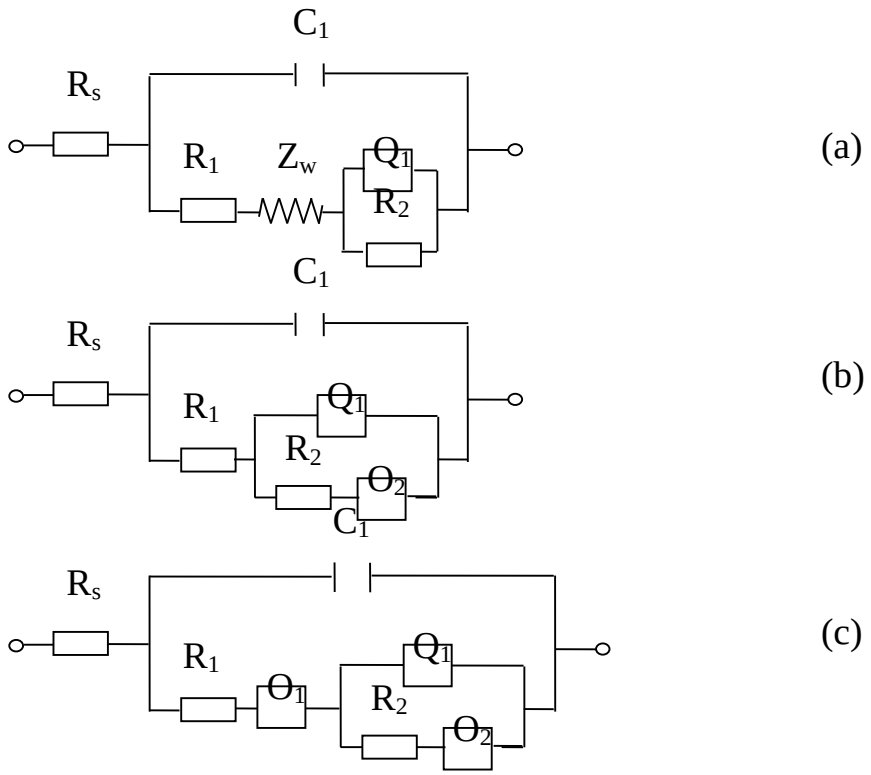

Figure 5. Equivalent circuits used to simulate the EIS plots in Figure 2C. (a) 0.8 V.(b) 0.85 V.(c) 0.92 V.

Nyquist plots in Fig. 2C are also simulated using corresponding equivalent circuits shown in Fig. 5. Where, R_s accounts for the uncompensated solution resistance from the reference electrode to the working electrode, C_1 and R_1 are the capacitance and charge transfer resistance of the electrochemical oxidation of aniline to radical on the Au electrode surface, respectively. Q_1 and R_2 are the double layer capacitance and charge transfer resistance which can be ascribed to the oxidation of PANI film. Z_w are the Warburg impedance due to the monomer diffusion in the solution. O_1 and O_2 are the resistance of finite diffusion on plane electrode. The absence of inductive element indicates the PANI films obtained in solution (iii) presents a more regular surface as reported by Hussain [41] in their study on the morphology of electrochemically synthesized PANI films.

Analogous conclusions can be obtained based on the plots shown in Fig. 2D' is similar to that in Fig. 2C'. The corresponding equivalent circuits used to simulate the Nyquist plots are also similar to that for Fig. 2C as shown in Fig. 6. Where R_s accounts for the uncompensated solution resistance between the reference electrode to the working electrode, C_1 and R_1 are the capacitance and reaction resistance of the electrochemical oxidation of aniline respectively. Q_1 and R_2 are the double layer capacitance and charge transfer resistance which can be ascribed to the oxidation of PANI film. Z_{w1} and Z_{w2} are the Warburg impedance due to the monomer diffusion in the solution. O is the resistance of finite diffusion on plane electrode. Based on the comparation of Fig. 5 and Fig. 6, it can be concluded that the electrochemical behavior of aniline in solution (iii) and solution (iv) is similar to each other, and the

difference between them is mainly reflected in the influence of diffusion on the electrode process.

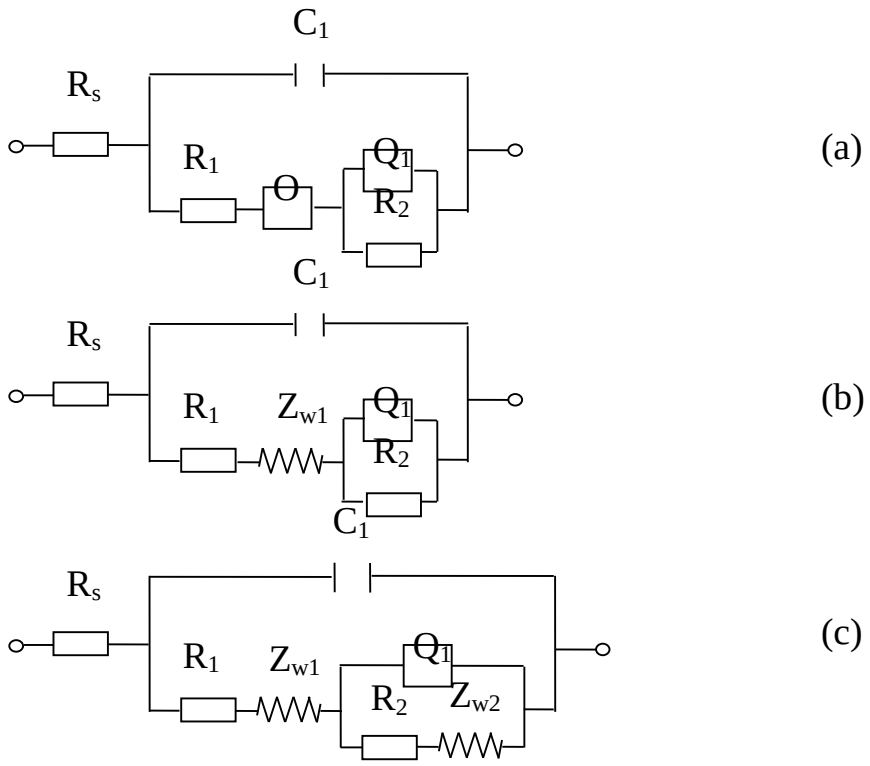

Figure 6. Equivalent circuits used to simulate the EIS plots in Figure 2D. (a) 0.82 V.(b) 0.85 V.(c) 0.92 V.

It is noteworthy that all Bode plots of solution (v) in Fig. 2E' show different characteristics from that of other solutions. All the plots show a inductive valley in high frequency region, which may be attributed to the catalysis of PO_4^{3-} on the electrochemical oxidation of aniline. We assume this effect may be associated with the trivalent of PO_4^{3-} ion, which made the formed PANI doped with PO_4^{3-} ion presented special properties [42, 43]. Meanwhile, all Bode plots show three time constants. The first one is corresponding to the catalysis of PO_4^{3-} on the oxidation of aniline. The second one is corresponding to the capacitance and resistance of the oxidation of monomer aniline. And the third one is corresponding to the double layer capacitance and charge transfer resistance which arise from the oxidation of PANI film.

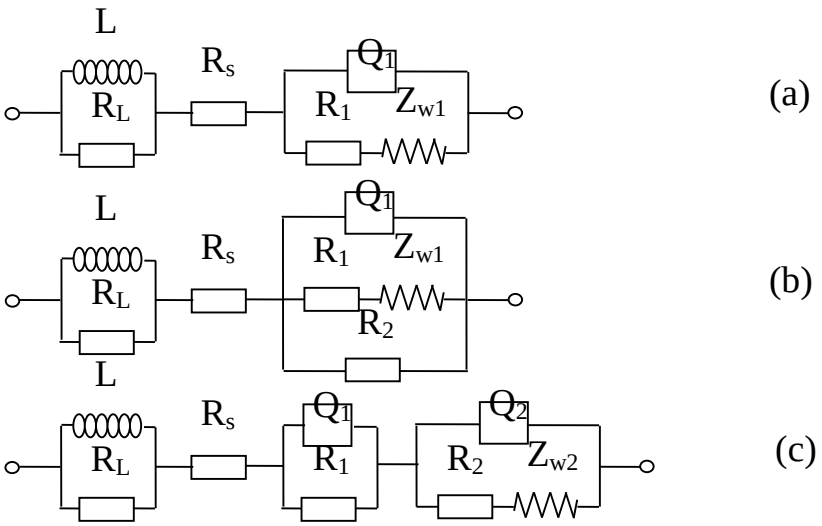

Figure 7. Equivalent circuits used to simulate the EIS plots in Figure 2E. (a)0.7V.(b)0.75V.(c)0.82V.

Nyquist plots in Fig.2E are also simulated using corresponding equivalent circuits shown in Fig.7, where L and R_L are related to the catalysis of PO_4^{3-} on the electrochemical oxidation of aniline. R_s accounts for the uncompensated solution resistance between the reference electrode to the working electrode, Q_1 and R_1 are the capacitance and reaction resistance of the electrochemical oxidation of aniline, respectively. Q_2 and R_2 are the double layer capacitance and charge transfer resistance which can be ascribed to the oxidation of PANI film. Z_{w1} and Z_{w2} are the Warburg impedance due to the monomer diffusion in the solution.

As a summary, electropolymerization of aniline in electrolyte containing different counter ions processed in similar way involving the oxidation of monomer aniline and PANI films. But the effect of uncompensated solution resistance, charge transfer resistance and double layer capacitance are different for each system. A catalytic effect of PO_4^{3-} was also revealed by EIS result, and that may explain the reason for the easiest electropolymerization in solution (v) as shown by CV.

It can also be obtained from the comparison of the radius of arcs on Nyquist plots recorded in each solution that the charge transfer resistances of electropolymerization of aniline are at low level in solutions containing NO_3^- and SO_4^{2-}, at middle level in solutions containing Cl^- and PO_4^{3-} and at high level in solution containing ClO_4^-, respectively.

EIS method has also often been used to study the power sources and electrochemical systems, especially supercapacitors. In order to investigate the capacitive behaviors of PANI film obtained in different solutions, PANI films were prepared by potentiostatic electropolymerizing on Au plate at 0.9 V in solution (i) ~ solution (iv) or at 0.7 V in solution (v) for 300 s, respectively. EIS measurements were conducted at open circuit potentials for PANI films electropolymerized in each solution, the testing results are shown in Fig. 8. As seen, the slopes of straight lines at low frequency region of all plots are high, which suggests fine capacitive behaviors of the systems.

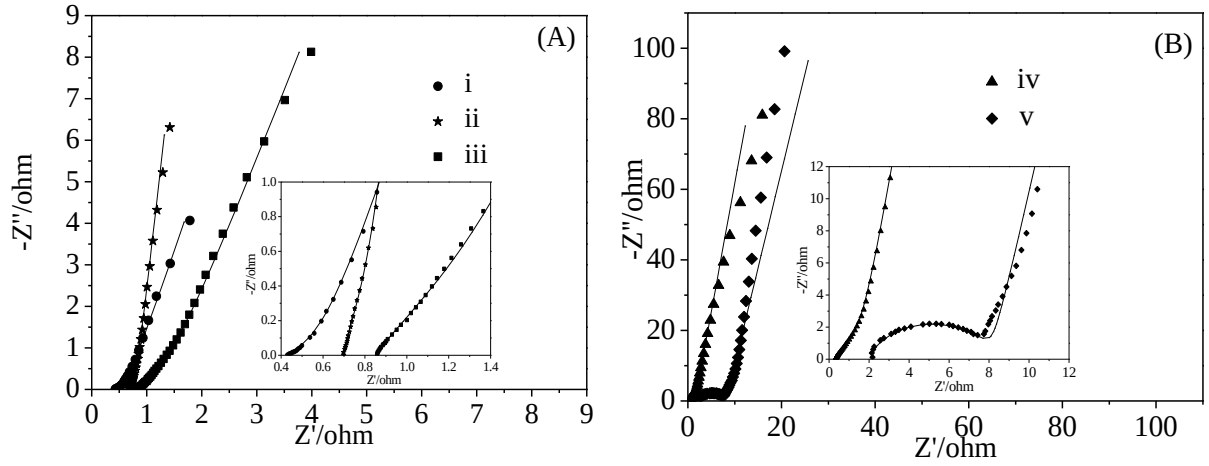

Figure 8. Nyquist plots of pAn film synthesized in different solutions at open circuit potentials. Points: tested data, line: simulated results.

EIS curves are usually fitted by an equivalent electric circuit for quantitative assessment of film properties. Several models have been proposed for discussing the electrical and capacitive behaviors of PANI films [31, 36, 40, 44-47]. We chose the equivalent circuit proposed by Ghenaatian to fit the experimental data due to it obtained the best fitting [44]. It is obvious that the circuit is consisted of a parallel combination of a charge transfer resistance (R_{ct}) with a double layer capacitance (Q_1) in series with a Faradic capacitance (Q_2), in addition to the solution resistance between the surface of the PANI film and the reference electrode (R_s) [44]. The corresponding electrical parameters were represented in Tab. 3. Conductivity and charge storage ability which can be reflected by the values of R_{ct} and C_2 in Tab.3, are the two important factors in fast redox systems, especially for supercapacitors [29, 36, 41]. So it can be obtained from Tab. 3 that PANI films synthesized in different solutions possess different capacitive behaviors.

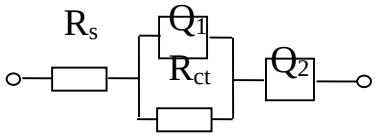

Figure 9. Equivalent circuit of the EIS plots in Figure 8.

Table 3. Electrical parameters for PANI film in different solutions obtained at OCP.

	$R_s(\Omega)$	$R_{ct}(\Omega)$	Q_1		Q_2	
			C_1(F)	n_1	C_2(F)	n_2
PANI/HNO_3	0.4318	0.2704	0.6817	0.4494	0.1968	0.8416
PANI/H_2SO_4	0.7009	0.0993	0.9315	0.8766	0.2106	0.9458
PANI/HCl	0.8468	0.6187	0.1840	0.5885	0.07963	0.8182
PANI/$HClO_4$	0.3234	1.2650	0.0572	0.7282	0.03915	0.9133
PANI/H_3PO_4	1.9200	6.216	0.00024	0.7641	0.00924	0.8854

The order of the R_{ct} value of PANI films obtained in solutions containing different counter-ions from high to low is: PANI/H_3PO_4 > PANI/$HClO_4$> PANI/HCl > PANI/H_2SO_4 > PANI/HNO_3. It means that the conductivity of PANI films from high to low is in the opposite order. The order of the C_2 value of PANI films obtained in different solutions from high to low is: PANI/H_2SO_4 > PANI/HNO_3 > PANI/HCl > PANI/$HClO_4$> PANI/H_3PO_4. It means that the charge storage ability of PANI films from high to low is in the same order. As a summarization, PANI/HNO_3 and PANI/H_2SO_4 show best capacitive behaviors, PANI/HCl and PANI/$HClO_4$ show capacitive behaviors at middle level, PANI/H_3PO_4 shows worst capacitive behavior.

4. CONCLUSIONS

Effects of counter-ions in electrolytes on electropolymerization behaviors and energy storage ability of obtained PANI films were discussed in this paper. As a result, the difficulty of electropolymerization of aniline in electrolytes containing different kinds of counter-ions from high to low is in the order: NO_3^-> SO_4^{2-}> ClO_4^-> Cl^-> PO_4^{3-}, while the rate of electropolymerization of aniline in electrolytes containing different kinds of counter-ions from high to low is in the order: SO_4^{2-}> NO_3^-> Cl^-> ClO_4^-> PO_4^{3-}. The charge transfer resistances of electropolymerization of aniline are at low level in solutions containing NO_3^- and SO_4^{2-}, at middle level in solutions containing Cl^- and PO_4^{3-}, at high level in solution containing ClO_4^-, respectively. The order of the conductivity of PANI films obtained in solutions containing different counter-ions from high to low is: PANI/HNO_3 > PANI/H_2SO_4> PANI/HCl > PANI/$HClO_4$ > PANI/H_3PO_4. . The order of the charge storage ability of PANI films obtained in different solutions from high to low is: PANI/H_2SO_4 > PANI/HNO_3 > PANI/HCl > PANI/$HClO_4$> PANI/H_3PO_4. PANI/HNO_3 and PANI/H_2SO_4 show best capacitive behaviors, PANI/HCl and PANI/$HClO_4$ show capacitive behaviors at middle level, PANI/H_3PO_4 shows worst capacitive behavior.

References

1. K. Doblhofer, R.D. Armstrong, *Electrochim. Acta,* 33 (1988) 453.
2. A. G. MacDiarmid, L. S. Yang, W. S. Huang, B. D. Humphrey,*Synth. Met.,* 18 (1987) 393.
3. J. Desilvestro, W. Scheifele, O. Haas, *J. Electrochem. Soc*., 139 (1992) 2727.
4. Y. Qiao, C. M. Li, S. J. Bao, Q. L. Bao, *J. Power Sources,* 170 (2007) 79.
5. J. Lu., K. S. Moon, B. K. Kim, C. P. Wong, *Polymer,* 48 (2007) 1510.
6. V. Gupta, N. Miura, *Electrochim. Acta,* 52 (2006) 1721.
7. J. H. Sung, H. J. Kim, K. H. Lee, *J. Power Sources,* 126 (2004) 258.
8. C. Meng, C. Liu, S. Fan, *Electrochem. Commun*., 11 (2009) 186.
9. M. R. Anderson, B. R. Mattes, H. Reiss, R. B. Kaner, *Science,* 252 (1991) 1412.
10. S. Kuwabata, C. R. Martin, *J. Membrane Sci*., 91 (1994) 1.
11. T. Hino, S. Taniguchi, N. Kuramoto, *J. Polym. Sci. Part A: Polym. Chem*., 44 (2006) 718.
12. S. Demoustier-Champagne, J. Duchet, R. Legras, *Synth. Met*., 101 (1999) 20.
13. J. Duchet, R. Legras, S. Demoustier-Champagne, *Synth. Met*., 98 (1998) 113.
14. A. M. P. Hussain, A. Kumar, *Bull. Mater. Sci.,* 26 (2003) 329.
15. V. Gupta, N. Miura, *Mater. Lett*., 60 (2006) 1466.

16. S. Bhadra, S. Chattopadhyay, N. K. Singha, D. Khastgir, *J. Appl. Polym. Sci*., 108 (2008) 57.
17. S. Xiong, Q. Wang, H. Xia, *Synth. Met.,* 146 (2004) 37.
18. R. V. Parthasarathy, C. R. Martin, *Chem. Mater*., 6 (1994) 1627.
19. G. Sauer, G. Brehm, S. Schneider, K. Nielsch, R. B. Wehrspohn, J. Choi, *J. Appl. Phys*., 91 (2002) 3243.
20. R. Nagarajan, S. K. Trypathy, J. Kumar, F. F. Bruno, L. A. Samuelson, *Macromolecules,* 33 (2000) 9542.
21. R. Nagarajan, W. Liu, J. Kumar, S. K. Tripathy, F. F. Bruno, L. A. Samuelson, *Macromolecules,* 34 (2001) 3921.
22. C. Nastase, F. Nastase, A. Dumitru, M. Ionescu, I. Stamatin, *Compos. Part A—Appl.* S., 36 (2005) 481.
23. F. Nastase, I. Stamatin, C. Nastase, D. Mihaiescu, A. Moldovan, *Prog. Solid State Ch*., 34 (2006) 191.
24. R. A. Barros, W. M. Azevedo, F. M. Aguiar, *Mater. Charact*., 50 (2003) 131.
25. P. K. Khanna, N. Singh, S. Charan, A. K. Viswanath, *Mater. Chem. Phys*., 92 (2005) 214.
26. A. F. Diaz, J. A. Logan, *J. Electroanal. Chem*., 111 (1980) 111 .
27. E. W. Paul, A. J. Ricco, M. S. Wrighton, *J. Phys. Chem*., 89 (1985) 1441.
28. G. Mengoli, M. T. Munari, P. Bianco, M. M. Musiani, *J. Appl. Polym. Sci*., 26 (1981) 4247.
29. W. F. Yang, H. Xu, Y.Y. Li, W. Wang, *J. Electron. Mater.,* 46 (2017) 4815.
30. A. Abd-Elwahed, R. Holze, *Synth. Met.,* 131 (2002) 61.
31. Q. L. Hao, W. Lei, X. F. Xia, Z. Z. Yan, X. J. Yang, L. D. Lu, X. Wang, *Electrochim. Acta,* 55 (2010) 632.
32. M. Lapkowski, E. Vieil. *Synth. Met.,* 109 (2000) 199.
33. H. J. Yang, A. J. Bard, *J. Electroanal. Chem.,* 339 (1992) 423.
34. D. E. Stilwell, S. M. Park, *J. Electrochem. Soc.,* 135 (1988) 2254.
35. Z. Mandic, L. Duic, F. Kovacicek, *Electrochim. Acta,* 42 (1997) 1389.
36. H. N. Dinh, V. I. Birss, *J. Electrochem. Soc.,* 147 (2000) 3775.
37. Y. Z. Li, Y. Yi, W. F. Yang, X. Q. Liu, Y. Y. Li, W. Wang, *J. Electron. Mater.,* 46 (2017) 1324.
38. W. Scheider, *J. Phys. Chem*., 79 (1975) 127.
39. O. Genz, M. M. Loherengel, J. W. Schultze, *Electrochim. Acta,* 39 (1994) 179.
40. M. Grzeszczuk, P. Poks, *J. Electrochem. Soc.,* 387 (1995) 79.
41. A. M. P. Hussain, A. Kumar, *Indian J. Phys.,* 79 (2005) 1033.
42. J. Dejeu, A. Cot, P. Rougeot, B. Lakard, S. Lakard, M. Gauthier, *Synth. Met.,* 276 (2021) 116757.
43. G. Boara, M. Sparpaglione, *Synth. Met.,* 72 (1995) 135.
44. H. R. Ghenaatian, M. F. Mousavi, S. H. Kazemi, M. Shamsipur, *Synth. Met.,* 159 (2009) 1717.
45. T. B. Hunter, P. S. Tyler, W. H. Smyrl, H. S. White, *J. Electrochem. Soc.,* 134 (1987) 2198.
46. C. Gabrielli, M. Keddam, N. Nadi, H. Perrot, *J. Electroanal. Chem.*, 485 (2000) 101.
47. K. Darovicki, J. Kawula, *Electrochim. Acta,* 49 (2004) 4829.